JOURNAL OF APPLIED ELECTROCHEMISTRY 24 (1994) 481–488

Dynamic analysis of charge transport in fluidized bed electrodes: Impedance techniques for electroactive beds

C. GABRIELLI, F. HUET, A. SAHAR

UPR15 du CNRS, Physique des Liquides et Electrochimie, Laboratoire de l'Université Pierre et Marie Curie, Tour 22, 4 place Jussieu, 75252 Paris Cedex 05, France

G. VALENTIN

Laboratoire des Sciences du Génie Chimique, ENSIC, Rue Grandville, Nancy, France

Received 12 March 1993; revised 25 October 1993

Impedance techniques are used to investigate the average dynamic behaviour of a fluidized bed of gold-coated beads in potassium ferri-ferrocyanide/NaOH solution. A transmission line is used as a model. The main features of the fluidized bed are correctly interpreted, especially the capacitive high frequency impedance related to the intermittent contacts between the particles. The use of a non-uniform transmission line is attempted in order to study the influence of a distance dependent charge transfer mechanism in the bulk of the fluidized bed.

1. Introduction

In a previous paper [1], it was shown that the average dynamic behaviour of a fluidized electroinactive bed can be described from the impedance measured between the current feeder and the reference electrode located above the bed. A description of charge transport in fluidized bed electrodes based on the model of Newman and Tobias [2] was proposed to explain the experimental results in terms of impedances. The main result obtained on the electroinactive system investigated (gold/NaOH interface) is the evidence for a capacitive/resistive contact impedance between the particles which leads to an extra parasitic overvoltage.

In this paper the previous model is applied to an electroactive bed where a redox reaction occurs between the gold-coated beads and the electrolyte.

2. Experimental results

The experimental arrangement of the fluidized bed is the same as in the previous paper [1]. The measurement of the potentials were made by means of a composite probe. The potential of the metallic phase, ϕ_m, was determined by a gold electrode of bead form and the potential of the electrolytic phase, ϕ_s, by a saturated calomel reference electrode. The impedance measurements were carried out using a frequency response analyzer (FRA Schlumberger 1250) and the experimental arrangement depicted in Fig. 1 where the fluidized bed is polarized by a potentiostat.

Before investigating the impedances which characterize the fluidized bed, preliminary studies involving current/voltage curves and potential distribution inside the fluidized bed were performed with 1 M NaOH electrolyte containing 0.015 M of potassium ferrocyanide and 0.001 M of potassium ferricyanide. The fluidized bed behaviour was tested in various regimes with the electrolysis current limited either by reaction kinetics or by mass transport of the electroactive species.

2.1. *Current voltage curves*

Figure 2 shows steady-state current/voltage curves, I/V (where $V = \phi_s(x) - \phi_m(0)$ with $x = 18\,\text{mm}$) obtained potentiostatically for various values of the electrolyte velocity, with the composite probe located 2 mm above the bed. When the bed was completely fluidized ($u \geqslant 1\,\text{cm s}^{-1}$) its height was about 16 mm. Therefore the local potential values corresponding to the current/voltage curve of Fig. 2 were taken at about 18 mm from the current feeder. At high velocity ($u = 1.4\,\text{cm s}^{-1}$), where the bed was completely fluidized, the current showed very large fluctuations and the average current was estimated by means of an oscilloscope.

These curves show a well defined diffusion limited current in the cathodic domain as the potassium ferricyanide had a much lower concentration than the potassium ferrocyanide. The limiting current increases as the electrolyte velocity increases, especially in the fixed bed situation. However, as soon as the bed becomes fluidized ($u = 1.4\,\text{cm s}^{-1}$), the plateau is less well defined and the limiting current increased more slowly than expected.

When the electrolyte velocity between the particles increased, the anodic current also increased so long as the bed remained motionless. However, as soon as the fluidization threshold was exceeded, the current diminished rapidly when the particles were separated and in motion. This feature showed that

0021-891X

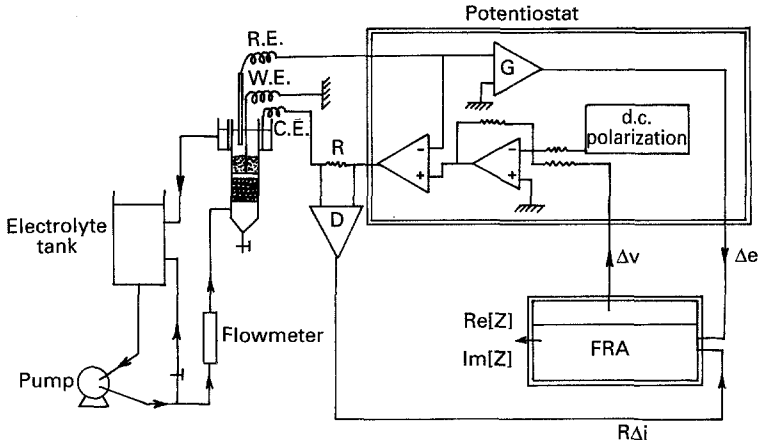

Fig. 1. Experimental arrangement used for impedance measurement. RE: reference electrode (composite probe): WE: working electrode (current feeder): CE: counter electrode.

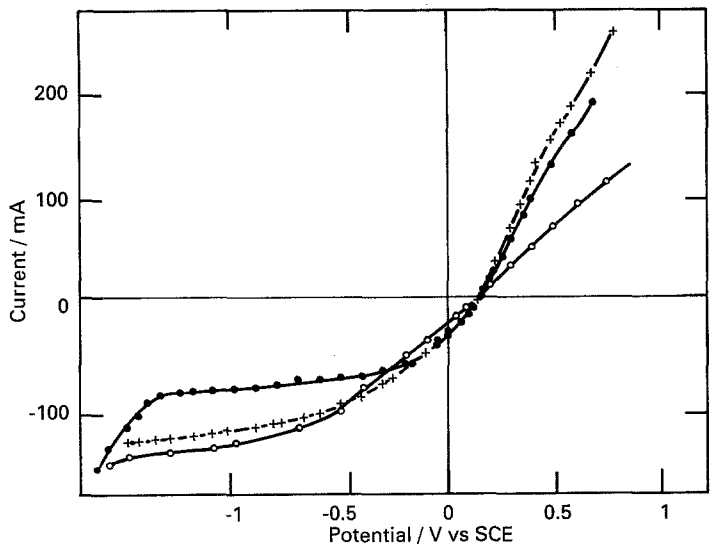

Fig. 2. Current/voltage curves of the fluidized bed for various values of the electrolyte velocity: (●) 0.25; (+) 0.45; (○) 1.4 cm s^{-1} for golden beads in 1 M NaOH containing 0.015 mol dm^{-3} of potassium ferrocyanide and 0.001 mol dm^{-3} of potassium ferricyanide.

an extra parasitic overvoltage was added when the bed was fluidized.

Figure 3 gives the solution potential $\phi_s(x) - \phi_m(0)$ for three points of the current/voltage curve; this potential was measured at various distances, x, from the current feeder at potential $\phi_m(0)$ and at various velocities when the bed was completely fluidized. These potential distributions are in agreement with the literature data [3, 5, 6].

2.2. *Impedance measurements*

Impedance measurements were carried out for several electrolyte velocities at three polarization points in the characteristic zones of the I/V curve: i.e. in the cathodic domain, in the anodic domain and at the equilibrium potential. When the measurements were carried out on the fluidized bed, it was not possible to perform measurements down to very low frequencies because of the current fluctuations.

2.2.1. Cathodic domain: Impedance measurements were carried out at −1 V vs SCE; at this potential the cathodic current is mass transport limited (Fig. 4(a)). As in the case of the NaOH 1 M solution alone [1], the resistive value obtained as the limiting value of the impedance at high frequency ($f \geqslant 10$ kHz), in the following termed the high frequency resistance, R_{HF}, increased when the bed was fully fluidized. Its variation is plotted in Fig. 4(b) against electrolyte velocity. For comparison the change in porosity versus electrolyte velocity was plotted in the same Figure.

On the other hand, the high frequency capacitive loop, hardly detected in the case of a still bed, was clearly observed when the bed was fluidized as in NaOH 1 M alone [1]. In the lower frequency range, this loop is followed by a diffusion impedance for the two bed states (still and fluidized). For the three electrolyte velocities, the frequency shift

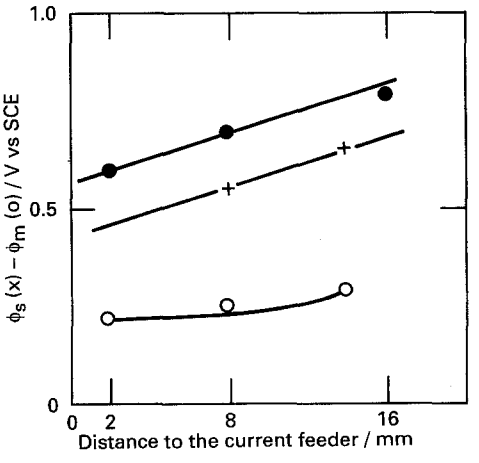

Fig. 3. Potential of the solution $\phi_s(x)$ against the distance x from the current feeder measured against the potential of the current feeder $\phi_m(0)$ in three points of current/voltage curve in the experimental conditions for which the bed is completely fluidized in the anodic region. $I = 50$ mA: (○) 0.98 cm s^{-1}; $I = 100$ mA : (+) 0.98 cm s^{-1}; (●) 1.27 cm s^{-1}.

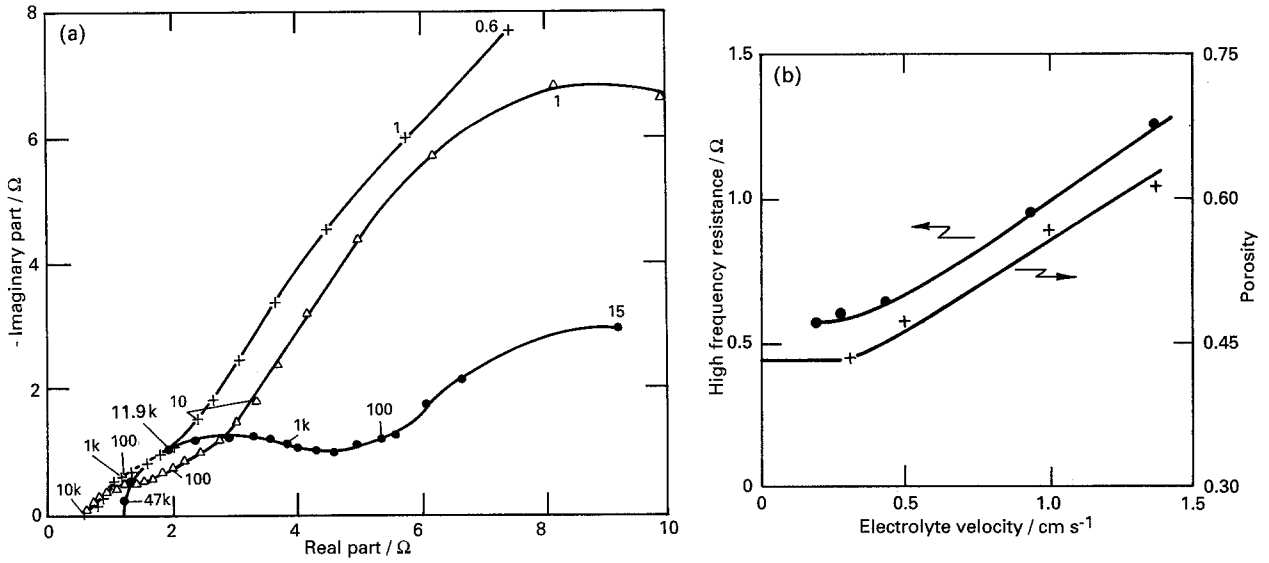

Fig. 4. (a) Impedance diagrams measured for various electrolyte velocities at potential −1 V vs SCE (cathodic domain) for (+) 0.09, (Δ) 0.44 and (●) 1.4 cm s^{-1} (frequencies in Hz). (b) Variation of the high frequency resistance and porosity of the bed against electrolyte velocity.

observed on this last loop had to be assigned to the decrease of the diffusion layer thickness due to the increase of the velocity, which diminished the diffusion time constant.

2.2.2. Anodic domain: Impedance measurements were carried out at 0.5 V vs SCE; at this potential the anodic current was partially mass transport limited for low electrolyte velocities and possibly not at all for high electrolyte velocities. Impedances were plotted in the complex plane in Fig. 5(a). It was noticeable that for a fixed bed (curve with Δ), the impedance showed two loops relatively well separated, the second one due to the diffusion of the reactive species. When the electrolyte velocity increased (curve with +), the bed, still being motionless, the following features were obtained: (i) a decrease, if not disappearance, of the diffusion loop, (ii) a slight increase in the high frequency resistance and (iii) a flattening of the impedance diagram. The high frequency capacitive loop still appeared clearly when the bed was totally fluidized (curve with ●) but it was followed by a smaller loop. Given its frequency range, this smaller loop may be related to the charge transfer mechanism because the electrolyte velocity was sufficiently fast

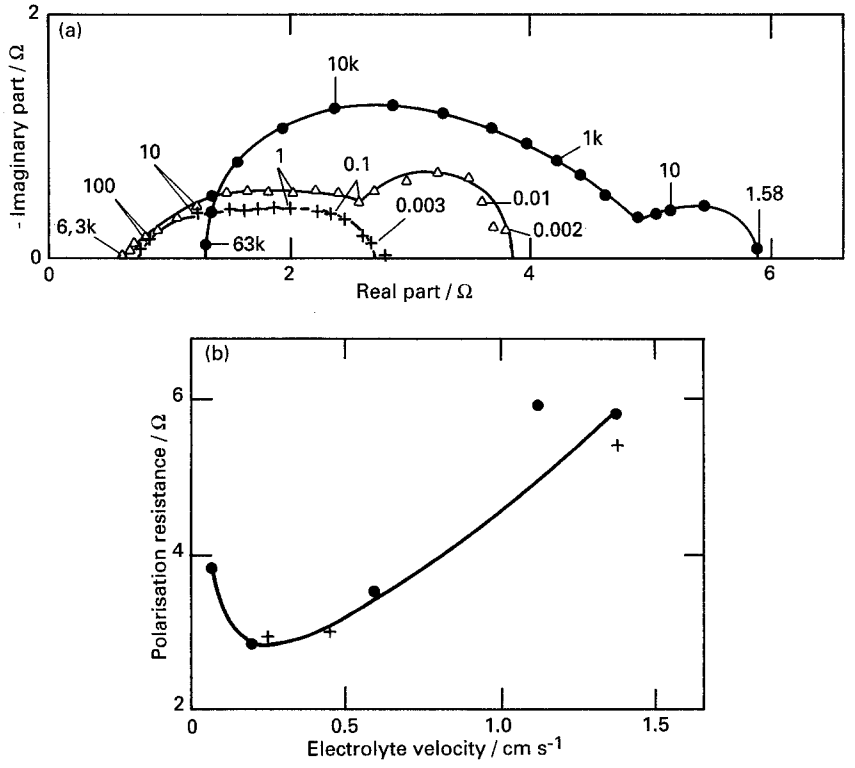

Fig. 5. (a) Impedance diagrams measured for various electrolyte velocities at potential 0.5 V vs SCE (anodic domain) for (Δ) 0.076, (+) 0.21 and (●) 1.13 cm s^{-1} (frequencies in Hz). (b) Variation of the polarisation resistance measured from the I/V curve (+) and the low frequency resistance obtained from the impedance (●) against electrolyte velocity.

in these experimental conditions that mass transport was not the rate limiting process.

The change of the low frequency resistance obtained from the impedance was plotted in Fig. 5(b) against electrolyte velocity, together with the polarization resistance obtained from the slope of the I/V curve. A good agreement was obtained between these two quantities. This showed, in these conditions, that the low frequency domain of the impedance was completely explored and that there was no extra loop hidden in the very low frequency range. The polarization resistance first showed a decrease when the electrolyte velocity began to increase with the bed still motionless. Then an increase induced by the extra voltage drop due to the intermittent contacts between the particles occurred as soon as the bed was fluidized.

When the electrolyte velocity was low, it was noticed that the high frequency part of the impedance diagram, measured on the fixed bed, was a straight line whose slope was close to one (45° inclination from the real axis). This fact had to be related to the spatial distribution of various parameters, particularly the potential, when the electrolyte was forced to flow through the fixed beads which formed a porous electrode.

2.2.3. Equilibrium potential: Impedances measured at zero current were plotted in Fig. 6. When the bed was motionless the impedance showed three loops; the low frequency one is assigned to diffusion. When the electrolyte velocity increased, the bed being still motionless, the low frequency loop decreased strongly; this led to a decrease in the low frequency resistance. When the bed was fluidized, the high frequency capacitive loop was still found. It was followed by a second loop which was partly concealed because of the vicinity of the time constant of the diffusion loop.

3. Discussion

In this work, the average dynamic behaviour of a fluidized electroactive bed was investigated by measuring the impedance of the bed. Very few experiments of this kind were carried out before as only Evans *et al.* published results using a nonpotentiostatic arrangement and a gain-phase meter [7, 8]. They performed experiments at only a few frequencies (0.1, 1 and 10 kHz) and they concluded that the resistivity is almost frequency-independent. However, the experimental results reported here show that the impedance diagram of the bed dramatically changed with the frequency, both in size and shape, in a broad frequency range (e.g. from 0.01 Hz to 100 kHz for the fluidized bed). These results demonstrate that the main elementary processes, which control the bed behaviour, can be separated. The experimental impedance diagrams show that the measurement of the apparent resistivity at a few frequencies can be misleading, as the faradaic processes began to have an influence at frequencies lower than 1 kHz.

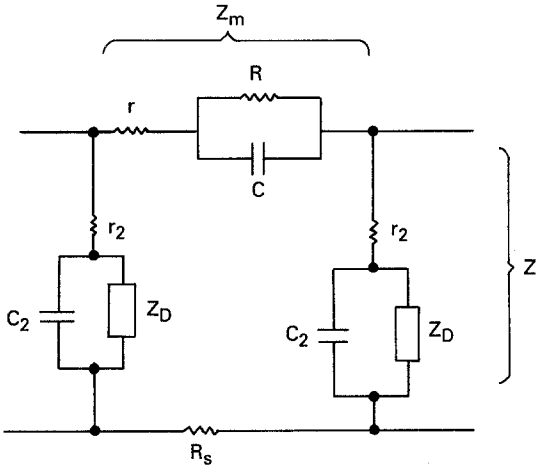

Fig. 7. Scheme of the transmission line used as a model of the fluidized bed for electroactive species showing: Z_m, contact impedance; Z, interfacial impedance; and R_s, solution resistance.

To interpret the experimental results predicted by the model proposed in the companion paper [1], the calculation of the impedance was carried out in various conditions.

First, the main results of the model of the average dynamic behaviour of a fluidized bed are recalled. In [1], it was shown that a fluidized bed electrode can be modelled by considering a transmission line whose impedance, Z_{fbe}, is given by

$$Z_{fbe} = \frac{Z_m R_s}{Z_m + R_s} L + \frac{(Z_m^2 + R_s^2)\cosh(\sqrt{(\gamma)}L) + 2Z_m R_s}{(Z_m + R_s)\sqrt{(\gamma)}\sinh(\sqrt{(\gamma)}L)} \quad (1)$$

where L is the bed height, $\gamma = (Z_m + R_s)/Z$, Z_m is the contact impedance between two particles, Z is the interfacial impedance between one particle and the electrolyte and R_s is the effective solution resistance.

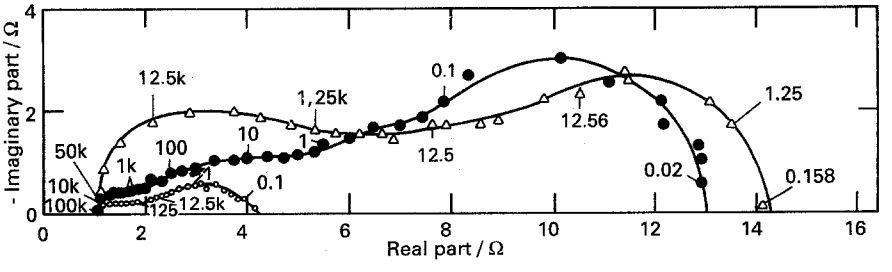

Fig. 6. Impedance diagrams measured for various electrolyte velocities at equilibrium potential for (●) 0.094, (○) 0.29 and (Δ) 1.09 cm s^{-1} (frequencies in Hz).

Table 1. Parameters values used for calculation of impedance diagrams given in Fig. 8

Quantity	*Fig. 8A(a)*	*Fig. 8A(b)*	*Fig. 8A(c)*	*Fig. 8B(a)*	*Fig. 8B(b)*	*Fig. 8B(c)*	*Fig. 8C(a)*	*Fig. 8C(b)*	*Fig. 8C(c)*
u/cm s^{-1}	0.089	0.44	1.36	0.094	0.289	1.085	0.076	0.2	1.13
L/cm	1.2	1.2	1.4	1.2	1.2	1.4	1.2	1.2	1.6
r_D/Ω cm	0.8	0.22	2.4	0.16	0.02	2.4	0.08	0.044	0.37
$k_b + k_f$/cm s^{-1}	5×10^{-3}	0.11	0.05	0.02	0.07	0.05	2.5×10^{-3}	3.6×10^{-3}	5.7×10^{-3}
δ_N/cm	0.012	0.0024	5.5×10^{-4}	0.012	2.4×10^{-3}	5.5×10^{-4}	0.012	6×10^{-3}	6×10^{-5}
C_2/F cm^{-1}	2	2×10^{-2}	1.5×10^{-4}	1.5×10^{-2}	1.5×10^{-2}	1.5×10^{-4}	2	1	0.11
r_2/Ω cm	5.6×10^{-3}	5.6×10^{-3}	6.5×10^{-2}	5.6×10^{-3}	5.6×10^{-3}	0.065	4.8×10^{-3}	4.8×10^{-3}	7.4×10^{-2}
R/Ω cm^{-1}	0	0.45	3.9	0	0.375	3.9	0	0.375	0.375
C/F cm	–	2×10^{-4}	4.7×10^{-6}	–	8×10^{-5}	4.7×10^{-6}	–	3.6×10^{-3}	1.1×10^{-5}
r/Ω cm^{-1}	0	0.45	0.434	0	0.375	0.43	0	0.375	0.375
R_s/Ω cm^{-1}	35	25	10	35	25	10	30	25	10

For electroactive species in the solution the elementary section of the transmission line used to perform the digital calculation of the impedance diagrams was given in Fig. 7 and was built from the following considerations. The contact impedance Z_m was identical to the situation where the gold beads were in contact with 1 M NaOH alone. Therefore, the contact impedance showed a capacitive feature, viz

$$Z_m = r + \frac{R}{1 + jRC\omega} \tag{2}$$

The interfacial impedance Z was obtained by taking into account a double layer capacitance C_2 and an electrolyte resistance r_2, in addition to the faradaic impedance Z_D, which showed a reaction-diffusion feature:

$$Z = r_2 + \frac{Z_D}{1 + jZ_D C_2 \omega} \tag{3}$$

where Z_D was the impedance of a transport limited charge transfer reaction across a diffusion layer of finite thickness δ_N such as

$$Z_D(\omega) = r_D\left\{1 + \frac{k_b + k_f}{\sqrt{(j\omega D)}}\tanh\left(\delta_N\sqrt{\left(\frac{j\omega}{D}\right)}\right)\right\} \tag{4}$$

where r_D is the charge transfer resistance, D the diffusion coefficient of the oxidized and reduced species (it is assumed that their diffusion coefficients were very close) and k_f, k_b are the forward and backward reaction rates of the redox reaction.

In a first step, this model (uniform transmission line) was tested by assuming that the various parameters are distance independent and in a second step the use of a nonuniform transmission line was attempted.

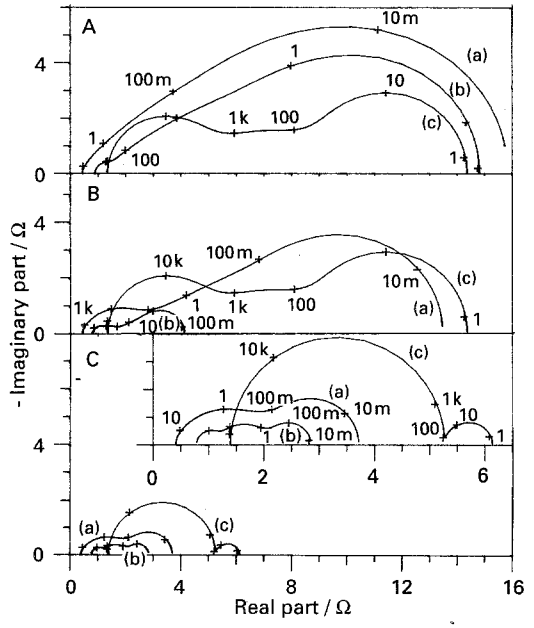

Fig. 8. Calculated impedance diagrams for the experimental conditions and parameters values described in Table 1. (A) Cathodic domain, (B) equilibrium potential and (C) anodic domain (frequencies in Hz).

3.1. *Uniform transmission line*

The impedance diagrams corresponding to the measurement conditions previously reported, i.e. cathodic domain, anodic domain and equilibrium potential were calculated for three electrolyte velocities. The numerical values affected to the parameters of the elementary section of the transmission line are given in Table 1 except the diffusion coefficient, D, which was kept constant for all the calculations and equal to $D = 7.7 \times 10^{-6}$ cm^2 s^{-1}.

For the anodic and cathodic domains, where the ohmic drop changed with the fluid velocity, it was necessary to change the rate constants with the velocity, in order to obtain a good agreement with the experimental results.

3.1.1. Cathodic domain: For the cathodic domain, the experimental shapes and frequency domains of the relaxations observed for various electrolyte velocities were again found by decreasing the thickness of the diffusion layer δ_N (which was equivalent to an increase of the electrolyte velocity) (Fig. 8(A)). The increase of the electrolyte velocity in the calculation was indicated by the increase of the high frequency resistance of the impedance diagrams in Fig. 8(A), (B) and (C). A nonzero contact impedance had to be introduced in order to reproduce the experimental results found in the high frequency range for the medium and large velocities, where the bed began to expand and was fully expanded.

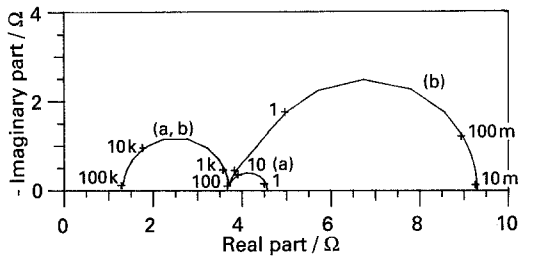

Fig. 9. Calculated impedance diagrams of a fluidized bed for (a) distance independent parameters and (b) distance dependence of the charge transfer resistance ($\gamma = 5$) with the following parameters: $r_0 = 0.375\,\Omega\,cm^{-1}$; $R_{s_0} = 10\,\Omega\,cm^{-1}$; $C = 1.1 \times 10^{-5}$ F; $R = 3.75\,\Omega\,cm^{-1}$; $C_2 = 0.11$ F; $r_2 = 0.074\,\Omega$ cm; $R_0 = 0.37\,\Omega$ cm; $n = 30$ (frequencies in Hz).

The capacitive high frequency loop was obviously absent for the totally fixed bed but as soon as the electrolyte circulated through the particles within the fixed bed this capacitive loop began to appear in the impedance and was clearly observed when the bed was fluidized. Therefore, when the bed was apparently motionless but electrolyte flowed through it, the particles oscillate slightly about their mean position, even for a low electrolyte velocity (e.g. $u = 0.1\,cm\,s^{-1}$). When the bed was fluidized this loop led to an extra parasitic overvoltage as a parasitic series resistance of the order of a few ohms was added to the classical transfer and diffusion overvoltages. This feature explained the tilting of the current/voltage curves towards more anodic potentials (Fig. 2) when the electrolyte velocity was increased beyond the threshold of the bed fluidization.

3.1.2. Equilibrium potential: For the equilibrium potential, three domains of relaxation were distinguished in the impedance diagrams, especially when the bed was fully fluidized (Fig. 8(B)). From the highest frequency range, the first loop was related to the intermittent contacts, the second loop to the reaction kinetics and the last loop, in the lowest frequency range, to the diffusion of the reactive species. The theoretical model given in [1] accurately reproduced the experimental results for various diffusion layer thicknesses (i.e. various fluid velocities).

3.1.3. Anodic domain: For the anodic domain and for low and medium velocities, it was still necessary to take into account the transport limitation to explain the shape of the diagrams which revealed a very low frequency loop (Fig. 8(C)). For a sufficiently high velocity of the electrolyte, where the transport was fast, the diffusion loop was not visible and the observed middle frequency loop was only due to the charge transfer mechanism. This feature showed that for low and middle velocities the total electrolysis current was partially kinetically controlled and partially mass transport controlled. For high velocities, the current was only kinetically controlled.

3.1.4. High frequency limit of the impedance: By replacing Z_m by r in Equation 1, the high frequency limit of the transmission line impedance is obtained (Equation 14 in [1]). From this quantity the value of the high frequency resistance, R_{HF}, is obtained for highly conducting beds where the metal matrix resistance, r, is much lower than the effective solution resistance, R_s:

$$R_{HF} \approx rL + \sqrt{(R_s r_2)}\,\mathrm{cotanh}\left(L\sqrt{\frac{R_s}{r_2}}\right) \qquad (5)$$

where the effective solution resistance, R_s, per free surface unit is related to the actual solution resistivity, ρ_s, and the porosity of the bed, ϵ. L is the bed height and r_2 is the electrolyte resistance of a sphere of radius a immersed in the solution [9]:

$$r_2 = \frac{\rho_s}{4\pi a} \qquad (6)$$

Figure 4(b) shows that the high frequency resistance, R_{HF}, follows the change in bed porosity when the electrolyte velocity increases. Therefore, R_{HF} measurement gives a way of estimating the experimental relationship between the solution resistivity, ρ_s, and the porosity of the bed, ϵ.

At intermediate frequencies, where the impedance Z_D is still short circuited by C_2, the low frequency extrapolation of the high frequency capacitive loop is given by replacing Z_m by $r + R$ in Equation 1 and

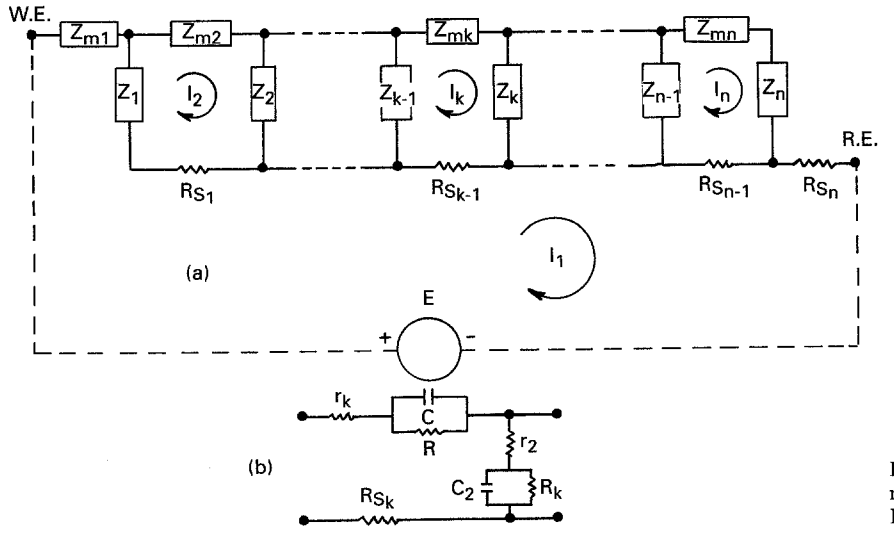

Fig. 10. Scheme of the nonuniform transmission line. (a) General scheme; (b) Elementary cell.

assuming $r + R \ll R_s$:

$$R_{HF_2} = (r+R)L + \sqrt{(R_s r_2)}\,\mathrm{cotanh}\left(L\sqrt{\frac{R_s}{r_2}}\right) \quad (7)$$

From the experimental value of R_{HF_2} the quantity, R, can be obtained. Therefore the contribution of the intermittent contacts between the beads to the parasitic overvoltage can be estimated.

3.2. *Nonuniform transmission line*

To see if the distance dependence of the parameters of the elementary section used in the transmission line may have an influence on the measured impedance the derivation of the impedance of a nonuniform transmission line was attempted (Appendix 1). This nonuniform transmission line analysis has been recently carried out for a simplified situation by D. D. MacDonald *et al.* [10].

An example of the impedance calculated from Equation A5 was given in Fig. 9(b), when the charge transfer resistance of the interface between a particle and the electrolyte was increasing with distance, due to the potential change in the case of a totally fluidized bed ($\alpha = \beta = 0$ and $\gamma = 5$ in Equation A5). For comparison, the impedance of the bed was calculated (Fig. 9(a)) when there was no distribution of the parameters ($\alpha = \beta = \gamma = 0$ in Equation A5). The high frequency loop was exactly the same with and without distribution of the parameter as the contact impedance was assumed distance-independent. However the low frequency loop was completely changed and took the shape of a diffusion impedance. This proved that some parameter distributions can lead to erroneous conclusions in the interpretation of the experimental results. Distance dependent particle concentrations, due to either contact impedance ($\alpha \neq 0$) or solution resistivity ($\beta \neq 0$) distributions, were tested. They also lead to deformation of the impedance diagrams. It was checked that the use of distance independent parameters ($\alpha = \beta = \gamma = 0$) with this discrete model (nonuniform line model) gave the same results as the continuous model (Equation 1).

4. Conclusion

The influence of the various phenomena which govern the dynamics of fluidized bed behaviour can be discerned in the impedance diagrams both for electroinactive [1] or electroactive beds. In addition to the loops related to the diffusion of the reactive species and to the faradaic reactions occurring at the gold coated particle surface, a capacitive impedance related to the intermittent contacts between the particles was observed in the high frequency range. Therefore it is necessary to perform impedance measurements in a wide frequency range to separate the main elementary processes which control the bed behaviour and to estimate their rates.

References

[1] C. Gabrielli, F. Huet, A. Sahar and G. Valentin, *J. Appl. Electrochem.* **22** (1992) 801.
[2] J. S. Newman and C. W. Tobias, *J. Electrochem. Soc.* **109** (1962) 1183.
[3] G. Valentin and A. Storck, *J. Chim. Phys.* **85** (1988) 281.
[4] B. J. Sabacky and J. W. Evans, *J. Electrochem. Soc.* **126** (1979) 1176.
[5] F. Goodridge and A. R. Wright, *in* 'Comprehensive Treatise of Electrochemistry', Vol. 6: 'Electrodics: Transport', (edited by E. Yeager, J. O'M. Bockris, B. E. Conway and S. Sarangapari), Plenum Press, New York (1983) p. 393
[6] T. Huh and J. W. Evans, *J. Electrochem. Soc.* **134** (1987) 308.
[7] *Idem, Ibid.* **134** (1987) 317.
[8] B. J. Sabacky and J. W. Evans, *Met. Trans.* **8B** (1977) 5.
[9] J. L. Anderson, *J. Electroanal. Chem.* **144** (1983) 403.
[10] D. D. MacDonald, M. Urquidi-MacDonald, S. D. Bhakta and B. G. Pound, *J. Electrochem. Soc.* **138** (1991) 1359.

Appendix 1

Derivation of the impedance of a nonuniform transmission line

The nonuniform transmission line used for the derivation of the impedance is shown in Fig. 10(a). The loop currents I_k can be calculated by solving numerically the linear system of equations obtained by writing the Kirchoff laws for each loop. For the kth loop:

$$Z_{k-1}(I_{k-1} - I_k) - Z_{m_k} I_k + Z_k(I_{k+1} - I_k) + R_{s_{k-1}}(I_1 - I_k) = 0 \quad (A1)$$

Equation A1 is valid for $2 \leqslant k \leqslant n$. For the first loop the following relationship is used:

$$Z_{fbe} I_1 = Z_{m_1} I_1 + Z_{m_2} I_2 + \cdots + Z_{m_k} I_k + \cdots + Z_{m_n} I_n + Z_n I_n + R_{s_n} I_1 \quad (A2)$$

and allows, Z_{fbe}, the total impedance of the nonuniform transmission line, to be calculated.

Therefore the following linear system of equations has to be solved to find the I_k/I_1 terms:

$$a_k \frac{I_K}{I_1} - b_k \frac{I_{k-1}}{I_1} - c_k \frac{I_{k+1}}{I_1} = d_k \quad 2 \leqslant k \leqslant n \quad (A3)$$

where

$$\left.\begin{aligned} a_k &= Z_{k-1} + Z_k + Z_{m_k} + R_{s_{k-1}} \\ b_k &= Z_{k-1} \\ c_k &= Z_k \\ d_k &= R_{s_{k-1}} \end{aligned}\right\} \quad (A4)$$

together with $I_0 = I_{n+1} = 0$.

Once the system of equation (Equation A3) is solved, the fluidized bed impedance is calculated from

$$Z_{fbe} = R_{s_n} + \sum_{k=1}^{n} Z_{m_k} \frac{I_k}{I_1} + Z_n \frac{I_n}{I_1} \quad (A5)$$

Various hypothesis can be tested. For a kinetically limited process whose elementary section is depicted in Fig. 10(b):

(i) if the particle concentration is distance-dependent,

either the contact impedance can be distance-dependent, i.e.

$$Z_{m_k} = r_k + \frac{R}{1 + \mathrm{j}RC\omega} \tag{A6}$$

where $r_k = r_0(1 + \alpha k/n)$; or the solution resistivity can be distance-dependent, i.e.

$$R_{s_k} = R_{s_0}(1 + \beta k/n) \tag{A7}$$

(ii) if the potential at the particle-electrolyte interface is distance-dependent, the transfer resistance can be distance-dependent, i.e.

$$Z_k = r_2 + \frac{R_k}{1 + \mathrm{j}C_2 R_k \omega} \tag{A8}$$

where $R_k = R_0 \mathrm{e}^{\gamma k/n}$